High Sea-Floor Stress Induced by Extreme Hurricane Waves

Hemantha W. Wijesekera, David W. Wang, William J. Teague, and Ewa Jarosz

Naval Research Laboratory, Bldg 1009, Code 7330,
Stennis Space Center, MS 39529

Abstract

Strong surface waves and currents generated by major hurricanes can produce extreme forces at the seabed that scour the seafloor and cause massive underwater mudslides. Our understanding of these forces is poor due to lack of concurrent measurements of waves and currents under these storms. Using unique observations collected during the passage of a category-4 hurricane, Ivan, bottom stress due to currents and waves over the outer continental shelf in the Gulf of Mexico was examined. During the passage of Ivan, the bottom stress was highly correlated with the wind with a maximum of about 40% of the wind stress. The bottom stress was dominated by the wave-induced stresses, and exceeded critical levels at depths as large as 90 m. Surprisingly, the bottom damaging stress persisted after the passage of Ivan for about a week, and was modulated by near-inertial waves.

Report Documentation Page

Form Approved
OMB No. 0704-0188

1. REPORT DATE **2010**	2. REPORT TYPE	3. DATES COVERED **00-00-2010 to 00-00-2010**
4. TITLE AND SUBTITLE **High Sea-Floor Stress Induced by Extreme Hurricane Waves**		5a. CONTRACT NUMBER
		5b. GRANT NUMBER
		5c. PROGRAM ELEMENT NUMBER
6. AUTHOR(S)		5d. PROJECT NUMBER
		5e. TASK NUMBER
		5f. WORK UNIT NUMBER
7. PERFORMING ORGANIZATION NAME(S) AND ADDRESS(ES) **Naval Research Laboratory,Bldg 1009, Code 7330,Stennis Space Center,MS,39529**		8. PERFORMING ORGANIZATION REPORT NUMBER
9. SPONSORING/MONITORING AGENCY NAME(S) AND ADDRESS(ES)		10. SPONSOR/MONITOR’S ACRONYM(S)
		11. SPONSOR/MONITOR’S REPORT NUMBER(S)

12. DISTRIBUTION/AVAILABILITY STATEMENT
Approved for public release; distribution unlimited

13. SUPPLEMENTARY NOTES

14. ABSTRACT

Strong surface waves and currents generated by major hurricanes can produce extreme forces at the seabed that scour the seafloor and cause massive underwater mudslides. Our understanding of these forces is poor due to lack of concurrent measurements of waves and currents under these storms. Using unique observations collected during the passage of a category-4 hurricane, Ivan, bottom stress due to currents and waves over the outer continental shelf in the Gulf of Mexico was examined. During the passage of Ivan, the bottom stress was highly correlated with the wind with a maximum of about 40% of the wind stress. The bottom stress was dominated by the wave-induced stresses, and exceeded critical levels at depths as large as 90 m. Surprisingly, the bottom damaging stress persisted after the passage of Ivan for about a week, and was modulated by near-inertial waves.

15. SUBJECT TERMS

16. SECURITY CLASSIFICATION OF:			17. LIMITATION OF ABSTRACT	18. NUMBER OF PAGES	19a. NAME OF RESPONSIBLE PERSON
a. REPORT **unclassified**	b. ABSTRACT **unclassified**	c. THIS PAGE **unclassified**	**Same as Report (SAR)**	**18**	

1. Introduction

Hurricanes can produce extreme forces at the ocean bottom, even on the outer continental shelf. Bottom stresses resulting from near bottom flows are less noticeable than surface winds and waves. These episodic wind events modify and control the near-bottom environment through resuspension and transport of sediments, and redistribution of organisms and chemicals. In the presence of strong surface waves, the combined current-wave stress is considerably larger than the bottom stress associated only with mean currents [e.g., *Grant et al.*, 1984; *Madsen et al*., 1993; *Cacchione and Drake*, 1982]. Stresses generated by the surface waves over the sea floor of the continental shelf have been often underestimated since wave heights under hurricanes were believed to exceed 20 m or so only in the 100-year storm events. Recently, an extreme wave with a crest-to-trough height of 28 m was measured under Hurricane Ivan and was not considered a rogue wave height but rather a common wave height that can occur under a major hurricane [*Wang et al.*, 2005]. Significant wave heights likely surpassed 21 m and maximum individual wave heights may have exceeded 40 m near the eyewall [*Wang et al.*, 2005].

The Gulf of Mexico (GOM) region provides nearly 30% of the United States oil supply and 20% of its natural gas. Hurricanes are major threats to the integrity of offshore operations over the GOM outer continental shelf. Significant damage can occur to underwater pipelines and to other underwater infrastructures such as oil and gas platforms [*Cruz and Krausmann*, 2008]. There are reportedly at least 50,000 km of pipeline on the seafloor of the GOM [MMS, 2006]. Damage to pipelines, which often is difficult to detect unless the damage is catastrophic, can be more costly to repair than damage to the superstructures on platforms. Major oil leaks from damaged pipelines could have irreversible impacts to the ocean environment. Improved understanding and accurate prediction of hurricane-induced bottom stresses on the seafloor area along hurricane paths can enable better engineering designs to reduce pipeline failures. However, understanding of hurricane-induced extreme bottom stresses is hampered by the lack of direct measurements of near-bottom flow generated by winds and waves under intense storms. Deployments of large numbers of instruments along hurricane tracks are not practically feasible. There are only a few reported wave and current measurements directly under the paths of historical hurricanes. For example, elevated bottom stress and sediment resuspension over the Mid-Atlantic-Bight shelf off the east coast of US were found during the passage of Hurricane Edouard in 1996 [*Dickey et al*., 1998; *Chang et al*., 2001]. The eye of the hurricane passed within 110 km of the mooring site when the maximum wind speed and wave height were about 20 m s^{-1} and 9 m, respectively, and the resuspension of sediments was up to 30 m above the seabed. The maximum bottom stress based on a current-wave interaction model [*Christoffersen and Jonsson*, 1985] was about 0.35 N m^{-2}.

Measurements of bottom pressures and full water-column current profiles were fortuitously made under the eye of Hurricane Ivan in 2004 by the Naval Research Laboratory (NRL) as part of the Slope to Shelf Energetics and Exchange Dynamics (SEED) project [*Teague et al*., 2007]. Six current-profiler moorings along with wave-tide gauges were deployed on the continental shelf at water depths ranging between 60 and 90 m near 29.4^{o}N, 88^{o}W (Figure 1). Ivan passed over the SEED mooring array on September 16 around 0000 UTC as a category-4 storm before making landfall near Gulf

Shores, Alabama [*Teague et al.*, 2007; *Powell et al.*, 1998]. The measurements indicated that significant wave heights exceeded 20 m; near-bottom wave-induced oscillatory currents were over 2 m s^{-1} [*Wang et al.*, 2005]; and bottom scours exceeded 0.3 m at the 60 m isobath [*Teague et al.*, 2007]. Extreme waves, currents, and scours as observed during Ivan are likely produced by other hurricanes.

The main objective of this paper is to quantify bottom stress over the continental shelf during the passage of Ivan. The seabed frictional coefficients and bottom stresses were evaluated from the observed near-bottom currents and wave-orbital velocities in combination with the wave-current boundary layer model [e.g., *Christoffersen and Jonsson*, 1985]. This study focuses on the growing and relaxation stages of the hurricane. During the growing stage of Ivan (between September 10 and 17, 2004), the coastal ocean was directly forced by accelerating winds from 10 to 50 m s^{-1}, and during the relaxation stage (between September 18 and 25, 2004), surface winds became weak but the circulation was dominated by wind-generated near-inertial currents [*Mitchell et al*., 2005]. The correlation of the bottom stress with the surface wind stress is also investigated.

2. Methods

A number of models have been formulated to evaluate wave-induced bottom stress [e.g., *Grant and Madsen*, 1979; *Trowbridge and Madsen*, 1984; *Christoffersen and Jonsson*, 1985; *Glenn and Grant*, 1987]. Some advanced models [*Trowbridge and Madsen*, 1984; *Glenn and Grant*, 1987] address complex seabed sediment conditions such as armoring and moveable beds. In the following we used a simple fixed flat-bed model described in *Christoffersen and Jonsson* [1985] (hereinafter CJ85), mainly because the exact nature of the seabed sediment conditions were not known during the passage of Ivan. CJ85 is similar to the most commonly-used model [*Grant and Madsen*, 1979], but utilizes an iterative approach for computing frictional coefficients based on bottom currents, wave statistics, and sediment grain sizes. CJ85 was used to evaluate bottom stress and sediment resuspension over the Mid-Atlantic-Bight shelf off the east coast of United States in the wake of Hurricane Edouard and Hortense in 1996 [*Dickey et al*., 1998; *Chang et al.*, 2001]. The selection of a particular model would not make a significant difference in the general conclusions presented here. However, the estimated bottom stress during the storm should be treated as a lower bound, since the bottom could be a movable bed, which tends to generate a higher-roughness scale than what was used in the fixed-bed representation of the critical bottom stress [e.g., *Madsen et al*., 1993]. Comparison of several wave-current boundary-layer models are given in [*Soulsby et al*., 1993].

The iterative procedure described in CJ85 computes the wave friction factor (f_w), the current friction factor (f_c), and then the combined current-wave stress (τ_{cw}) on the sea bed, where $\tau_{cw} = 0.5 f_w \rho u_w^2 m$; ρ is the density of sea water; m describes the relation between the current and the wave, and is a function of f_w , f_c , wave orbital velocity (u_w), current velocity (u_c), and angle between the current and the wave; f_c depends on the Nikuradse roughness (k_N) [*Nikuradse*, 1933], the apparent roughness (k_A), and the height of the current boundary layer (h). The bottom stress due to the mean current is: $\tau_c = 0.5 f_c \rho u_c^2$. The combined current-wave-dissipation rate (ε_{cw}) and the current-dissipation rate (ε_c) were estimated using the following relationships:

$\varepsilon_{CW} = (\tau_{CW} / \rho)^{3/2} / (\kappa\, z)$ and $\varepsilon_{C} = (\tau_{C} / \rho)^{3/2} / (\kappa\, z)$, where z is the height from the bottom, and κ is the von Karman constant (0.4).

The near-bottom flow field was composed of a background mesoscale component driven by a basin-scale wind stress curl in addition to low-frequency currents ranging from inertial to sub-inertial flows [*Teague et al.*, 2007]. The most-significant bottom currents were directly wind driven with superimposed high-frequency oscillatory currents driven by surface waves and swells. Bottom stresses and dissipation rates were computed from background currents and wave-orbital velocities at the seafloor. The bottom wave-orbital velocities were estimated from 512-s burst-sampling records of wave-induced dynamic pressure measurements at 0.25 m above the bottom [*Wang et al.*, 2005] based on linear wave theory. Ocean currents at 0.25 m above the bottom were approximated by extrapolating near-bottom velocities from acoustic Doppler current profilers (ADCPs) while assuming the constant stress layer with a logarithmic velocity profile (i.e., "law of the wall") extends from the seabed to the depth of the first measured velocity above the ADCP. Typically the thickness of the wall boundary layer is about 10% of the thickness of the bottom mixed layer. During the passage of Hurricane Ivan, the current structure was found to be frictionally driven with overlapping surface and bottom boundary layers [*Mitchell et al.*, 2005] suggesting that the entire water column over the shelf was either weakly stratified or well mixed. Therefore, a 6- to 9-m-thick wall boundary layer is expected near the vicinity of the sea floor. The moorings rested on a sandy seabed with grain sizes varying from 0.06 mm to 1 mm with a median size of about 0.3 mm [*Sawyer et al*., 2001]; therefore k_N was approximated to be about 0.3 mm. The alignment angles between the currents and wave orbital velocities were not known, and therefore, the currents and waves were assumed to be in the same direction and the alignment angle was set to zero for the computations. Since wave statistics were only sampled every 8 hours, estimates of τ_{cw} and ε_{cw} were limited to 3 times per day. The bottom currents from the ADCP were sampled at 15-minute intervals, and therefore τ_c and ε_c were computed at a higher sampling rate by interpolating 8-h estimates of f_c into the ADCP sampling rate. By following *Madsen et al.* [1993], the wave-orbital velocity was approximated as the root-mean-square amplitude of a sinusoidal wave, where $u_w = \sqrt{2}\sigma_u$, and σ_u is the standard deviation of orbital-velocity fluctuations based on the 512-s burst-sampling record of pressure at 0.25 m above the bottom [*Wang et al.*, 2005]. The surface wind field over mooring locations was constructed by combining NDBC buoy winds with Ivan post storm wind analysis products [*Wang et al.*, 2005; *Powell et al.*, 1998].

3. Observations

A dramatic increase in bottom stress and dissipation rate was found at all six mooring locations during the passage of Ivan. At the 60-m isobath, the current-wave stress (τ_{CW}) was enhanced by two orders of magnitude (Figure 2c) and the current-wave dissipation rate (ε_{CW}) was enhanced two to three orders of magnitude (Figure 2d) as the wind speed accelerated from 10 m s^{-1} to 50 m s^{-1}, during which wave-orbital bottom velocity intensified from O(mm s^{-1}) to O(1 m s^{-1}) (Figure 2a, b). At the 90-m isobath, wave-orbital velocities were relatively weak, background currents were strong (Figure 2g), and the current-wave stress was a factor of two smaller than that at the 60-m isobath (Figure 2c,h). Peak bottom stresses at moorings M1 to M6 were 0.47, 0.58, 0.84, 0.62, 0.48, and 0.34 N m^{-2}, respectively. Some of the differences in current-wave stresses at different mooring locations were related to the undersampling of wave-orbital velocities at an 8-h interval and depth dependence of wave statistics. Out of the six moorings, M3, which was located to the right of Ivan's path (Figure 1), had the strongest bottom stress, largest wave-orbital velocity (Figure 2b,c) and the largest surface-wave height of about 28 m [*Wang et al*., 2005]. There was an increase in background stress levels following the hurricane; the current stress (τ_C), averaged over the mooring array, prior to Ivan was $7\text{x}10^{-3}$ N m^{-2} [$1\text{x}10^{-6}$, $4\text{x}10^{-2}$] while that stress after Ivan was $30\text{x}10^{-3}$ N m^{-2} [$20\text{x}10^{-6}$, $27\text{x}10^{-2}$], where minimum and maximum stresses are given in the brackets.

The ADCP echo intensity (Figure 2e,j) reflects the concentration of particles in the water column [*Deines*, 1999]. Therefore the timing and the duration of the resuspension of sediments (during which $\tau_{cw} >$ the critical stress) can be identified from the echo intensity. The observed critical stress is consistent with the spiking of echo intensity. The resuspension occurred as the wind speed exceeded ~ 15 m s^{-1} and lasted for two days over both 60-m and 90-m isobaths. After the passage of Ivan, the resuspension continued at the 60-m isobath, and was modulated by near-inertial waves (Figure 2e), but it was considerably weaker at the 90-m isobath (Figure 2j). The intensity of the ADCP echo was enhanced up to 25 m above the instrument, implying that sediments were resuspended to about 25 m above the seabed (Figure 2e,j).

The relationship between bottom stress (τ_{cw}, τ_c) and wind speed (U_{10}) during the growing stage of the hurricane was studied by averaging bottom stresses into appropriate bins as a function of the wind speed (Figure 3). The impact of surface waves on the bottom stress was not important for winds less than 8 m s^{-1}. There was a rapid build up in τ_{cw} as U_{10} increased from 10 m s^{-1} to 15 m s^{-1}. The growth of τ_{cw} slowed down for U_{10} >

20 m s^{-1}, and τ_{CW} was approximately proportional to U_{10}^2. τ_C was also proportional to U_{10}^2 for most of the wind record. On average τ_C was a factor of 4 smaller than τ_{CW} based on the wave-orbital velocity, $u_w = \sqrt{2}\sigma_u$ (Figure 3). The current-wave stress can be approximated as $\tau_{CW} \approx 4\times10^{-4} U_{10}^2$ for winds higher than 15 m s^{-1}, which in turn implies that $\tau_{CW} \approx C\tau_S$, where τ_S is the surface wind stress, and the proportionality constant, $C = 4\times10^{-4} / \rho_{air} C_D^S$; ρ_{air} is the density of air, and C_D^S is the surface drag coefficient. For $C_D^S = (1.5-2.5)\times10^{-3}$ (13), C is ~ 0.15 - 0.2. Sensitivity of τ_{CW} to the strength of the orbital velocity was examined by choosing the wave-orbital velocity as significant wave-orbital velocity (u_{ws}), where, $u_{ws} = 2\sigma_u$, and the wave-orbital velocity as maximum wave-orbital velocity (u_{WM}). It is clear from Figure 3 that τ_{CW} is highly sensitive to the magnitude of the wave-orbital velocity chosen. The estimate of τ_{CW} for the maximum wave-orbital velocity, u_{WM} is about a factor of 2 larger than that for the root-mean-square velocity, $\sqrt{2}\sigma_u$.

4. Summary and Discussion

During the passage of Ivan, the bottom stress, energy dissipation rate, and resuspension of sediment were controlled primarily by dissipative processes induced by surface waves, whereas during the relaxation stage of Ivan, wave-orbital velocities became small and the bottom stress, dissipation rates, and resuspension of sediments were determined by the observed bottom current. The strongest stresses occurred to the right of the storm path. Bottom stresses exceeded critical levels on the outer continental shelf at depths as large as 90 m. Bottom damaging stresses occurred during the passage of the storm and for about a week after storm passage. The bottom stress associated with the ocean currents peaked at wind speeds of about 30 m s^{-1} and then may actually have decreased as the wind speed increased, paralleling the surface drag reduction at high winds [*Jarosz et al*., 2007; *Powell et al*., 2003]. The current-wave induced bottom stress continued to increase as the wind speed increased, and was about 15%-20% of the surface wind stress, where $u_w = \sqrt{2}\sigma_u$. The maximum stress based on the maximum wave-orbital velocity was found to be as large as 40% of the surface wind stress. On average, bottom stresses induced by ocean bottom-current interactions with ocean surface-wave-related currents were a factor of 4 larger than the bottom stresses attributed to ocean bottom currents alone.

The occurrence of critical bottom stresses on the outer shelf must be considered in the engineering design of structures on the bottom and in determining where pipe lines should be buried and not just laid on top of the ocean floor. Some climate models have predicted an increase in the frequency of intense hurricanes as the climate warms [*Bender et al*., 2010]. The cumulative effects of enhanced bottom stresses and associated transport of large quantities of sediment along the shelf edge could be a trigger mechanism for a slumping or mass-wasting event at the shelf break.

Acknowledgments. This work was supported by the Office of Naval Research as part of the NRL's basic research project SEED under program element grant 0601153N. Comments given by Jim Richman were greatly appreciated.

References

Bender, M. A., T.R. Knutson, R.E. Tuleya, J.J. Sirutis, G.A. Vecchi, S.T. Garner, and I.M. Held (2010), Modeled impact of anthropogenic warming on the frequency of intense Atlantic hurricanes, *Science*, *327*, 454-458.

Cacchione, D. A., and D. A. Drake (1982), Measurements of storm generated bottom stress on the continental shelf, *J. Geophys. Res.*, *87*, 1952-1961.

Chang, G. C., T. D.. Dickey, and A. J. Williams III (2001), Sediment resuspension over a continental shelf during Hurricane Edouard and Hortense, *J. Geophys. Res.*,*106*, 9517 -9531.

Christoffersen, J. B., and I. G. Jonsson (1985), Bed friction and dissipation in a combined current and wave motion, *Ocean Eng.*, 12, 387-423.

Cruz, A. M., and E. Krausmann, (2008), Damage to offshore oil and gas facilities following hurricane Katrina and Rita: An overview, *J. Loss Prevention Process Ind.*, *21*, 620-626.

Deines, K. L., (1999), Backscatter estimation using broadband acoustic doppler current profilers, IEEE 6th working conference on current measurement, San Diego, 249-253, DOI:10.1109/CCM.1999.755249.

Dickey, T. D., G. C. Chang, Y. C. Agrawal, A. J. Williams, III, and P. S. Hill (1998), Sediment resuspension in the wakes of Hurricane Edouard and Hortense, *Geophys. Res. Lett.*, *25*, 3533-3536.

Glen, S. M., and W. D. Grant (1987), A suspended sediment stratification correction for the combined wave and current flows, *J. Geophys. Res.*, *92*, 8244-8264.

Grant, W. D., A. J. Williams III, and S. M. Glenn (1984), Bottom stress estimates and their predication on the northern California continental shelf during CODE-1: The importance of wave-current interaction, *J. Phys. Oceanogr.*, *14*, 506-527.

Grant, W. D., and O.S. Madsen (1979), Combined wave and current interaction with rough bottom, *J. Geophys. Res.*, *84*, 1797-1808.

Jarosz, E., D.A. Mitchell, D.W. Wang, and W.J. Teague (2007), Bottom-up determination of air-sea momentum exchange under a major tropical cyclone, *Science*, *315*, 1707-1709 .

Madsen, O. S., L. D. Wright, J. D. Boon, and T. A. Chisholm (1993), Wind stress, bed roughness and sediment suspension on the inner shelf during an extreme strom event, *Cont. Shelf Res.*, *13*, 1303-1324.

Mitchell, D. A., W.J. Teague, E. Jarosz, and D.W. Wang (2005), Observed currents over the outer continental shelf during Hurricane Ivan, *Geophys. Res. Lett.*, 32, doi:10.1029/2005GL023014.

Minerals Management Service (MMS) (2006), Pipeline damage assessment from Hurricanes Katrina and Rita. Technical Report No. 448 14183, 104pp.

Nikuradse, J., Stromungsgesetz in rauhren rohren, vdi-forschungsheft 361 (1933). (English translation: Laws of flow in rough pipes), 1950. Technical report, NACA Technical Memo 1292. National Advisory Commission for Aeronautics, Washinton, DC.

Powell, M. D., S. H. Houston, L. R. Amat, and N. Morisseau-Leroy (1998), The HRD real-time hurricane wind analysis system, *J. Wind Eng. Ind. Aerodyn.*, *77&78*, 53-64.

Powell, M. D., P. J. Vickery, and T. A. Reinhold (2003), Reduced drag coefficient for high wind speeds in tropical cyclones, *Nature*, *422*, 279-283.

Teague, W. J., E. Jarosz, D.W. Wang, and D.A. Mitchell (2007), Observed oceanic response over the upper continental slope and outer shelf during Hurricane Ivan, *J. Phys. Oceanogr.*, 37, 2181-2206.

Trowbridge, J. H., and O. S. Madsen (1984), Turbulent wave boundary layers, 1, Model formulation and first-order solution, *J. Geophys. Res.*, *89*, 7989-7997.

Sawyer, W. B., C. Vaughan, D. Lavoie, Y. Furukawa, N. Carnaggio, J. Maclean, and E. Populis (2001), Report No. NRL/MR/7430-01-8548, Naval Research Laboratory, Stennis Space Center, Miss..

Soulsby, R. L., L. Hamm, G. Klopman, D. Myrhaug, R. R. Simons, and G. P. Thomas (1993), Wave-current interaction within and outside the bottom boundary layer, *Coastal Engineering*, *21*, 41-69.

Wang, D. W., D.A. Mitchell, W.J. Teague, E. Jarosz, and M.S. Hulbert (2005), Extreme waves under hurricane Ivan, *Science, 309*, 896-896.

Figure Captions

Figure 1. Path of Ivan (dashed red line). The crosses denote the center of Ivan for the time marked in red. Mooring locations at 60-m and 90-m isobaths are marked in solid circles (M1-M6). The yellow triangle is the National Data Buoy Center (NDBC) buoy 42040. Contours indicate bathymetry in meters. The translation speed of the hurricane was about 6 m s^{-1}.

Figure 2.Observations at M3 (left panels) and M6 (right panels) mooring locations. Time series of (a, f) 10-m wind speed U_{10} in m s^{-1} and radial distance to Ivan's center (black) in kilometers [*Powell et al*., 1998]. (b, g) Root-mean-square estimate of wave-orbital speed, $u_W = \sqrt{2}\sigma_u$ (red dots), where σ_u is the standard deviation of orbital-velocity fluctuations based on the 512-s burst-sampling record of pressure, and ADCP currents u_c (black line)

at 0.25 m above the bottom. Units are in m s^{-1}. (c, h) Combined current-wave stress τ_{CW} (red dots) and current stress τ_C (black line) in N m^{-2}. (d, i) Estimated current-wave dissipation rate ε_{CW} (red dots) and current dissipation ε_C (black line) at 0.25 m above the bottom. Units are in W kg^{-1}. (e, j) ADCP echo intensity as function of height (H) in meters from the bottom

Figure 3. Mean stress at 0.25 m above the bottom vs wind speed U_{10} during the growing stage of Ivan. The bottom stress based on mean current (u_c) is the solid black line with diamonds. The combined current-wave stress τ_{CW} based on bottom orbital-velocities: $u_w = \sqrt{2}\sigma_u$, significant wave-orbital velocity $u_{WS} = 2\sigma_u$, and maximum orbital-velocity, u_{WM} are marked in dots (red), squares (blue), and open circles (magenta) , respectively. Error bars are given by the thin red vertical lines and denote maximum and minimum values of τ_{CW} for $u_W = \sqrt{2}\sigma_u$. The dashed black and red lines are not mathematical fits to the data, but represent $\tau = 10^{-4} U_{10}^2$ (black), $\tau = 4 \times 10^{-4} U_{10}^2$ (red).

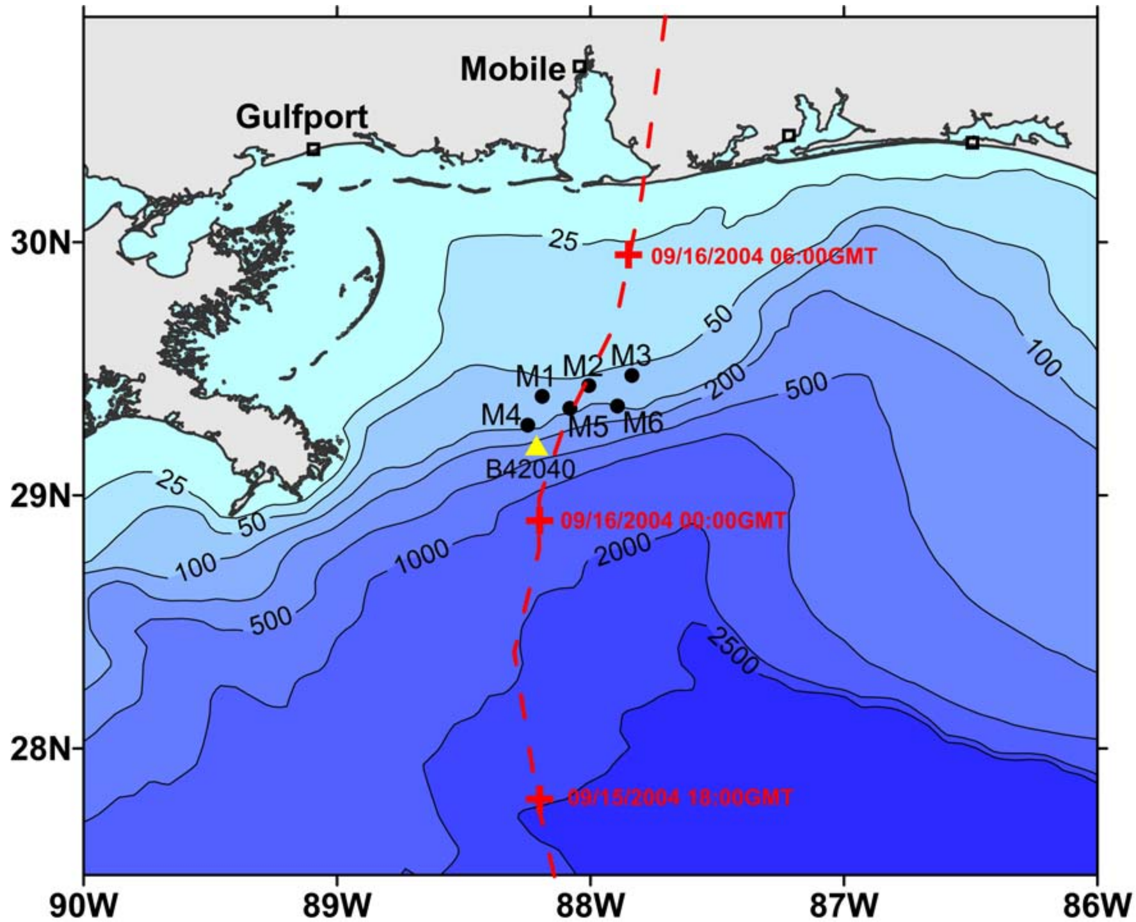
Mobile
Gulfport
30N
29N
28N
90W
89W
88W
87W
86W
25
50
100
200
500
1000
2000
2500
M1
M2
M3
M4
M5
M6
B42040
09/16/2004 06:00GMT
09/16/2004 00:00GMT
09/15/2004 18:00GMT

Figure 1

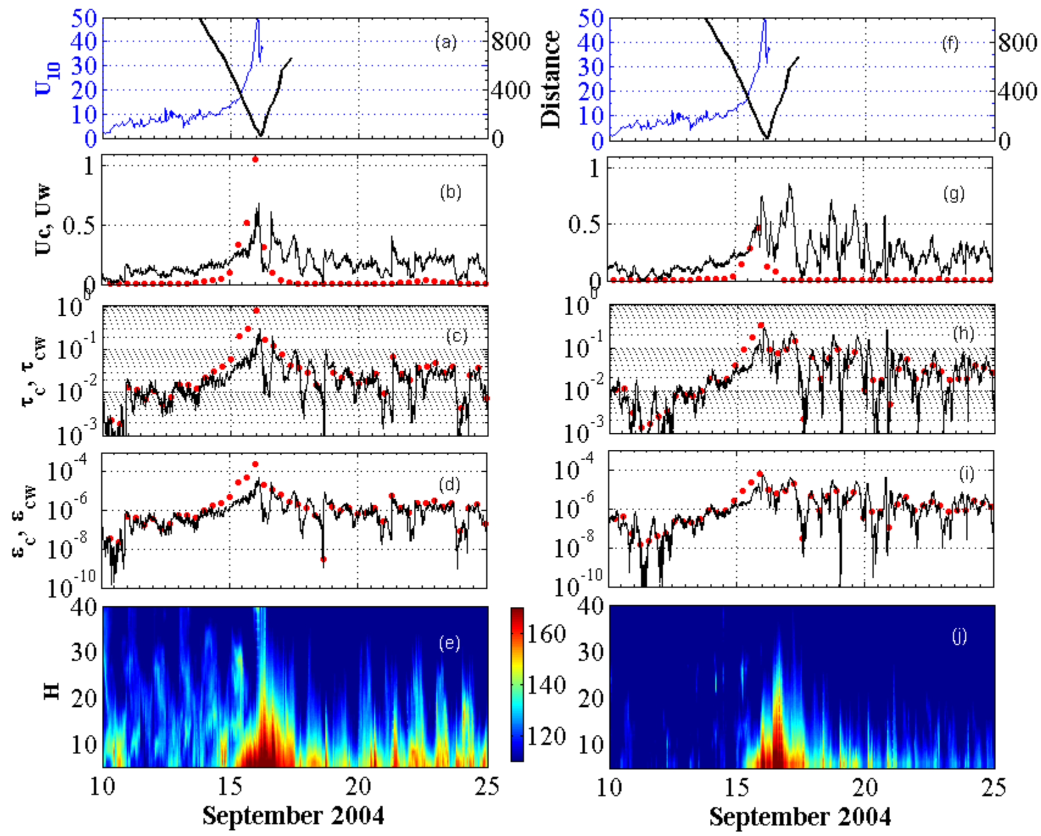
(a)
(b)
(c)
(d)
(e)
(f)
(g)
(h)
(i)
(j)
U_{10}
Distance
Uc, Uw
τ_c, τ_{cw}
ε_c, ε_{cw}
H
September 2004
September 2004

Figure 2

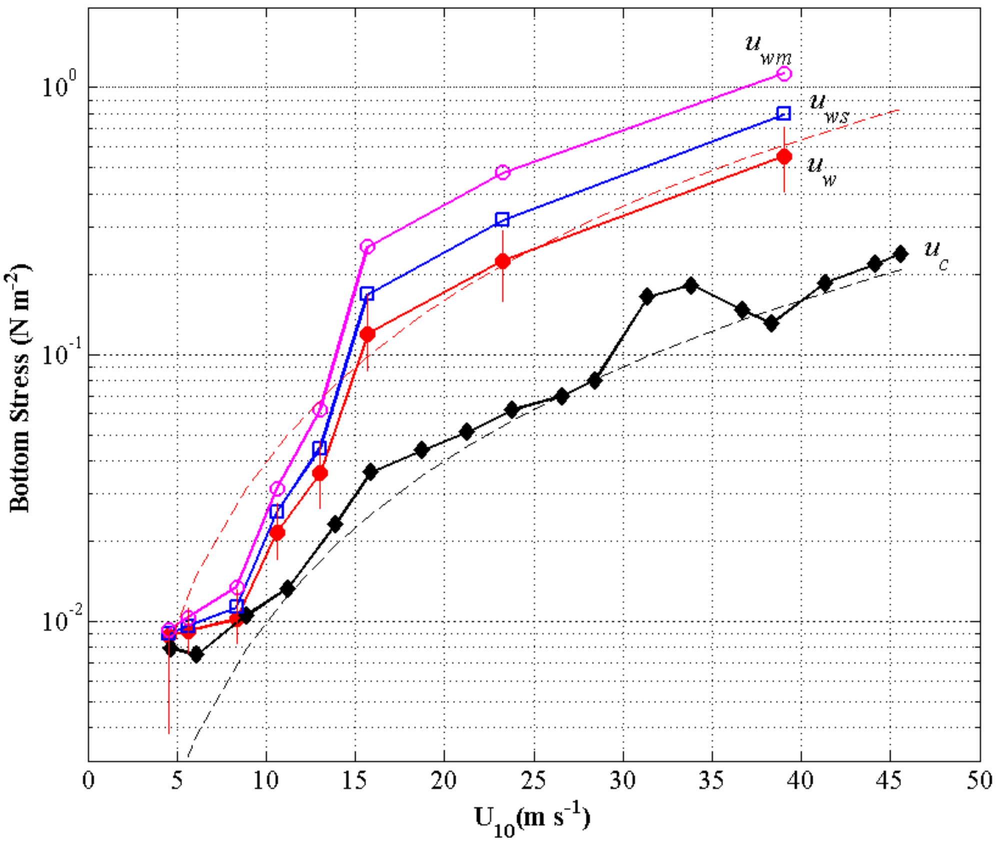

Bottom Stress (N m^-2)
U_10 (m s^-1)
10^0
10^-1
10^-2
0
5
10
15
20
25
30
35
40
45
50
u_wm
u_ws
u_w
u_c

Figure 3